INSULATION POLLUTION ESTIMATION IN THE FIELD: ULTRASOUND AND AUTO-ASSOCIATIVE ARTIFICIAL NEURAL NETWORKS

T. V. Ferreira[1]*, A. D. Germano[2], E. G. Costa[1], M. R. B. Pereira[3], R. N. Dias[4]
[1]Federal University of Campina Grande, Brazil
[2]Technischen Universität München, Germany
[3]Companhia Hidro Elétrica do São Francisco, Brazil
[4]TermoPernambuco S.A., Brazil
*Email: <tarso@dee.ufcg.edu.br>

Abstract: This work presents improvements in an insulation pollution estimation system. Such system proved functional under laboratory conditions, and extracts spectral information from the ultrasonic noise emitted by the corona discharges that occur in electric equipment. Then, it correlates the compacted spectral information with degrees of pollution previously defined. To achieve the classification, Auto-Associative Artificial Neural Networks are employed. Eight different insulation structures, from eight equipments were chosen for inspection. An inspection routine was defined, so all equipments had their ultrasonic sounds recorded in the same order, and from about the same point. The results show that the method suffers influence from the humidity, since it changes the ultrasound spectrum. On the other hand, this effect can be minimized if the database that is used to train the Auto-Associative Artificial Neural Networks is sufficiently diversified.

1 INTRODUCTION

Due to its unquestionable importance and overtime working on electrical systems, insulation was, and will be, the object of several studies. Thus, methods to monitor these devices have been developed and refined, as a reliable way to predict failures in isolation and prevent significant losses.

The most widely used method of monitoring is visual inspection, due to its low operating cost. However, for pollution detection, visual inspection is usually imprecise, having a high likelihood of false positive or false negative, depending on various factors such as type of pollution, humidity, electric field configuration, etc.

In this paper, we aim to add reliability to the Ultrasonic (US) pollution estimation of electrical insulation, in the field. For this, we used Auto-Associative Artificial Neural Networks (AAANN), which are able to correlate the ultrasonic spectra emitted by the insulations to its pollution degree. To achieve an efficient extraction of attributes, reducing the data volume from the US samples and allowing the use of AAANN, the Subband Spectral Centroid Energy Vectors (SSCEV) algorithm was employed.

2 ULTRASONIC INSULATION MONITORING

The inspection of insulation employing acoustic noise is based on a mechanical effect of electric discharges. The corona discharges that occur in the vicinity of polluted insulators result in localized and virtually instantaneous release of energy. This energy produces heat, noise in various acoustic and ultrasonic audible frequencies, and electromagnetic noise. The amplitude of an acoustic wave created by a single discharge is proportional to the square root of the mechanical energy released in the discharge [1].

Many researchers consider ultrasonic inspection of insulators an unreliable method [2]. This mistrust is adequately based mainly on human subjectivity inherent in the diagnosis, since the individual in charge of the insulation diagnosis may commit misjudgements. These mistakes can happen due to insufficient training or experience, but their causes are beyond the scope of this work. Thus, the occurrence of false positives or false negatives is high enough to discourage the use of the technique.

Still, some researchers have been addressing the issue, producing remarkable results. Studies published in recent decades indicate the feasibility of using acoustic emission signals as indicators of pre-failure situations [3]. In Table 1, some of the most significant works on this theme, developed in the last years, can be seen.

The proposed technique differs from others already published by allying, all at once, several advantages; for example, aid for decision making, and rapid and noninvasive inspection. It also employs low-cost and simple management equipment. These goals can be achieved by employing intelligent algorithms for spectral compression, with great ability to reject unwanted noise in the extraction of ultrasonic signal attributes. This algorithm is a modified version of another algorithm, originally proposed for speech recognition by [4]. The implemented modifications allow the SSCEV to process ultrasound, instead of voice signals, among other adaptations. The combination of the processed US spectra and AAANN significantly contributes to reduce the uncertainties in the decision making, when compared to the decision making performed by humans.

Table 1: Evolution of insulations US monitoring techniques.

Year	Researcher(s)	Contribution
1939	Kimura *et al.*	Experimented with crystal microphone immersed in oil to detect corona in EA and alternating voltage [5].
1964	Leslie & O'Beirne	Developed Coronaphone, the first equipment to perform the diagnosis of transmission lines based on EA [6].
1968	Dawnson *et al.*	Estimated the dominant frequency ranges for different disruptive distances [7].
1991	Yang & Dumont	Demonstrated the feasibility of US noise classification by Artificial Neural Networks (ANN) [8].
1996	Auckland *et al.*	Performed experiments to measure and record acoustic emissions (AE) in cables, bushings, porcelain insulators and equipments with oil tank, creating a database for ANN training [9].
2001	Abdel-Salam *et al.*	Determined how to classify ultrasonic noises coming from two different sources: surface discharges on polluted insulators and loose conductors tips [10].
2001	Boczar	Employed spectral analysis techniques to classify partial discharge coming from AE, using predefined arrays and contact sensors [11].
2008	Pei *et al.*	Proposed a method for real-time monitoring of pollution deposited on insulators, based on acoustic emissions [12].

3 THEORETICAL FRAMEWORK

3.1 Subband Spectral Centroid Energy Vectors

Originally, the Subband Spectral Centroid Histograms (SSCH) method was proposed for speech recognition applications and its most important feature might be considered its robustness against background noise. The computational cost is comparable to that demanded by other methods with similar purposes, such as *cepstral* coefficients [13]. Thus, since the SSCEV and SSCH have several similarities in the first steps of computation, SSCEV also shows the same advantages.

For illustration purposes, the process of SSCEV calculation from an USAE signal is shown in Fig. 1. This US sample has been registered from insulators from a 230 kV tower. Since the US has been processed by the detector, the ultrasonic band is represented in an audible range. In Fig. 1a, the 1 second length ultrasound sample is shown. In Fig. 1b, the estimated FFT from the US sample is plotted. Fig. 1c shows two different resulting SSCEV: the red one has a higher compression rate, and resulted in a poorly detailed vector composed of only 12 elements (sub-bands); the blue one has a lower compression rate, which results in a detailed vector composed of 40 elements.

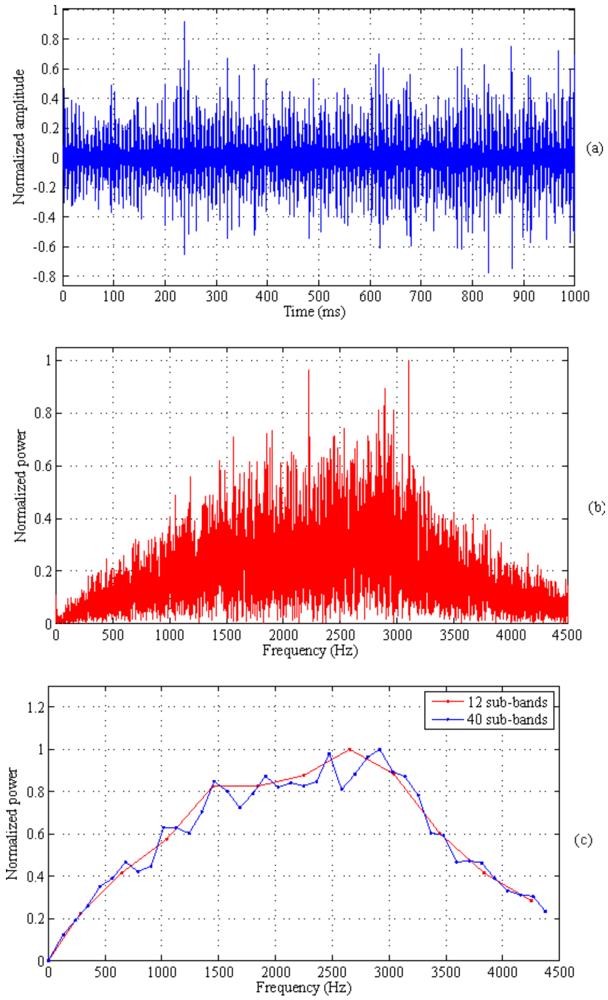

Fig. 1. SSCEV calculation from an USAE signal; (a) Processed ultrasound sample (1 second); (b) Estimated FFT obtained from the ultrasound sample; (c) Two examples of resulting SSCEV, with different compression rates.

The steps for SSCEV computing are described below:

i. For each USAE file recorded, the spectrum is calculated through Fast Fourier Transform (FFT);

ii. Then, the spectrum is divided in several subbands, through the application of rectangular superposed band-pass filters;

iii. The centroid localization (C_H) for each subband is calculated by using (1):

$$C_H = \frac{\sum_{k=0}^{N-1} H_m(k) \cdot P(k)}{\sum_{k=0}^{N-1} P(k)}, \quad (1)$$

where: *P(k)* = estimated spectrum (p.u.)
$H_m(k)$ = vector of frequencies (Hz)
N = samples into the filter;

iv. The energy associated to each centroid is calculated through (2):

$$E_c = \sum_{k=C_H-\delta \cdot N}^{C_H+\delta \cdot N} P(k) \quad (2)$$

where: δ = range in the neighborhood of the centroid.

The SSCEV element energy is then calculated within the range defined by δ.

3.2 Auto-Associative Artificial Neural Networks

The generalization ability of ANN is very welcome in the classification tasks, as well as its capability to adapt to new situations. This means that even if an US sample in the test case is not very similar to the samples used during training, there is still significant probability that the ANN will classify correctly.

The implemented ANN architecture is an Auto-Associative Artificial Neural Networks. It is a parallel composition of some classic Multilayer Perceptrons (MLP) [14], as can be seen in Figure 2.

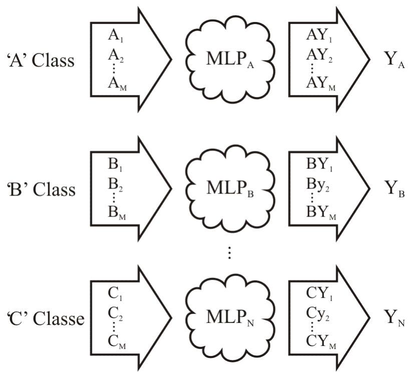

Fig. 2. Implemented AAANN.

In training, validation and testing of RNA, the percentage of 70%, 15% and 15% from the database, were respectively employed. The training was conducted with the Resilient Propagation algorithm [15], which is an evolution of the classical method, Backpropagation [16]. Each MLP inside the AAANN has three layers, which is a good compromise between accuracy and computational cost. The activation function chosen is the hyperbolic tangent, which allows the network to propagate negative values, providing a more equalized training through the layers [17].

Besides the obvious differences in terms of topology, the AAANN differs from the MLP in the way of specialized training for each subnet that compose it. The MLP_A, for example, only meet the samples of Class A; MLP_B know only Class B samples, and so on. More than that, the expected output after processing each subnet is the proper sample of entry, i.e. considering zero training error, we must have (3):

$$[A_1, A_2, \ldots, A_M] = [AY_1, AY_2, \ldots, AY_M] \quad (3)$$

In other words, each sub-network inside AAANN is an expert in one class; and in its output tries to emulate the same sample the input received.

When training and validation is completed, the testing starts. Every time a new sample has to be classified, it will be presented to all subnets. If a subnet is specialized in a different class from the one the sample belongs to, it cannot imitate the input sample in its output, generating a large error between input and output. Otherwise, the error is numerically small. Calculating the energy of the errors of all sub-networks, and comparing them to each other, it is concluded that the pattern in question belongs to the class of the subnet that generated less energy error. As the classes are composed of hundreds of patterns, the correct classifications of each sub-network are counted within the total testing group, so we have a probabilistic answer.

Besides the advantage of providing answers in terms of probabilities, the AAANN do not need counter-examples to conduct the training. So, the possibilities of output of the subnets are not exclusive, i.e., a sample can belong two or more subnets. This behaviour is illustrated in Figure 3.

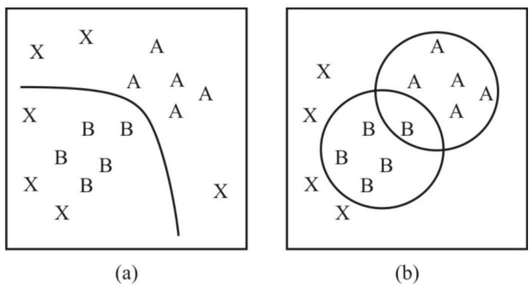

Fig. 3. Decision boundaries formed by training (a) an MLP and (b) two Auto-Associative Neural Networks on examples from classes A and B. Xs denote non-class examples [18].

4 METHODS

Aiming to verify the versatility of the technique, measurement campaigns were performed at two different facilities: in Campina Grande 2 substation (SECG2), which belongs to the Eletrobrás São Francisco Hydroelectric Company (Chesf); and in the TermoPE substation (SETPE), which belongs to TermoPernambuco S.A. Both substations operate in 230 kV.

Nine different types of equipments were chosen for inspection.

i. Anchor insulation string (SECGD);
ii. Circuit Breaker (SECGD);
iii. Switch (SECGD);
iv. Current Transformer (CT, SECGD);
v. Potential Transformer (PT, SECGD);
vi. Insulating column (SECGD);
vii. ZnO surge arrester (SECGD);
viii. Tower insulator string (SECGD);
ix. Circuit Breaker (SETPE).

Items (i) to (vii) and (ix) are station type equipment, and the inspection distance was approximately 6 m. Item (viii) is an insulator string operating in a tower of a transmission line. In this case, the insulator string is about 15 m away from the ultrasound detector.

The ultrasonic detector employed in both laboratory and field tests was an Ultraprobe 2000 MPH, which detects the ultrasonic and converts it into an audible frequency range (20 Hz < f < 3 kHz), without compression. The detector field of view is 15°, using the recommended module.

An inspection routine was defined, so all the equipment had their US recorded in the same order, and from about the same point. Before the US acquisition, relative humidity (RH) and temperature (Te) were registered. In order to capture a wider variety of situations of pollution, RH and Te, inspections were performed weekly in SECGD, for 15 weeks. The atmospheric conditions in SECGD during these weeks can be seen in Fig. 4.

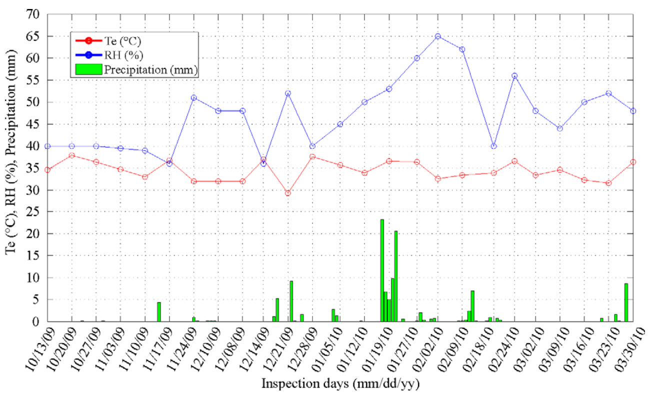

Fig. 4. Atmospheric conditions in the inspection days, in SECGD.

The inspections in SETPE occurred on two dates, and the atmospheric conditions are shown in Table 2.

Table 2: Data from measurements taken at RU SE Thermocouple.

Date	Te (°C)	RH (%)	Precipitation (mm)
09/29/2010	28,1	52,0	-
02/01/2011	38,8	38,3	139

Beyond the intense precipitation between the inspections in SETPE, an artificial washing with de-mineralized water was performed in late December/2010.

A data acquisition system was used to digitalize and store the audio. The sampling rate used was once again 44,000 samples per second. The registered audio was divided into smaller files, so that each of them would represent one pattern to the AAANN. Later, the SSCEV algorithm was applied, and all the patterns of all of the classes were used in the AAANN training, validating and testing.

5 RESULTS AND DISCUSSION

Once the VECSE were ready for AAANN training, it was also necessary to define how the database would be processed. So, three approaches were defined.

5.1 Approach 1

Samples obtained in 12/28/2009 (Te = 37.6 °C; RH = 40%, Class A) and in 02/18/2010 (Te = 33.9 ° C; RH = 40%, ClassB) were compared. Supposedly, these patterns are easily separable, since the first inspection occurred before the period of intense rainfall (19 to 27 January 2010) and the other was afterwards. The data was acquired in SECGD equipments (items i to viii). In Table 3, the second and third columns show the amount of test samples from a determined class, properly allocated. For the second line, i.e., (Circ. Breaker, right insulation), 2.35% of the test patterns of Class A were misclassified as Class B, and 0.78% of the Class B test patterns were misclassified as Class A.

Table 3: SECGD results for Approach 1.

Equipment	Class A hits (%)	Class B hits (%)
Anchor insulation string	100,00	100,00
Circ. Breaker (Right insulation)	97,65	99,22
Circ. Breaker (Left insulation)	99,80	100,00
Switch (moving contact)	100,00	100,00
Switch (fixed contact)	97,65	99,02
CT	99,41	99,80
PT	100,00	99,80
Insulating column	100,00	100,00
ZnO surge arrester	100,00	100,00

For illustration purposes, all the SSCEV for the anchor insulation string can be seen in Fig. 5, plotted superposed.

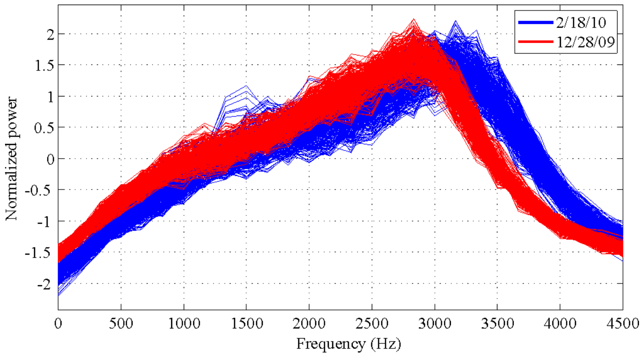

Fig. 5. SSCEV for the tower insulator string (Approach 1).

5.2 Approach 2

The audio obtained from the insulator strings from a tower arm were used in this approach. Due to the distance of inspection, this case is expected to be the most difficult. The AAANN trained with samples obtained from inspections in 12/21/2009 and 02/24/2010, which are separated by the rainy season (see Fig. 4). After training, the AAANN was tested with samples from all inspections produced between 10/13/2009 and 02/24/2010. The objective is to test the capacity of the network to associate pre-rain measurements (polluted insulation) with day 10/13/2009 (Class A), and post-rain (washed insulators) with day 02/24/2010 (Class B). In other words, it is evaluated whether it is possible to classify different levels of pollution by training the network only with samples obtained in borderline pollution level situations. The data was acquired in SECGD equipments (items i to viii). The results are shown in Table 4 (each inspection date shall be associated with a single class, so the columns have complementary values).

Table 4: SECGD results for Approach 2.

Date	Class A hits (%)	Class B hits (%)
10/13/09	99,93	0,07
10/20/09	100	0
10/27/09	99,33	0,67
11/03/09	**28,78**	**71,22**
11/10/09	95,47	4,53
11/17/09	95,03	4,97
11/24/09	**1,71**	**98,29**
12/10/09	99,7	0,3
12/08/09	99,7	0,3
12/14/09	100	0
12/21/09	100	0
12/28/09	**98,74**	**1,26**
01/05/10	1,85	98,15
01/12/10	44,66	55,34
01/19/10	1,71	98,29
01/27/10	0,67	99,33
02/02/10	14,24	85,76
02/18/10	0	100

The darkened regions in Table 4 determine the expected behavior of AAANN, and the red lines highlight the situations where the expected behavior did not occur. The errors may have occurred because of the humidity influence, among other issues not yet determined. Further investigation is needed to clarify these cases, and measurement errors cannot be discarded. Globally, however, the classification of pollution standards from borderline situations was successful in 13 of the 16 cases.

5.3 Approach 3

The samples came from the two measurements presented in Table 2. The pollution levels are significantly different. The humidity was not equal. The data was acquired in SETPE circuit breakers (item ix). Results are shown in Table 5, and the hit counting is similar to the one presented in Approach 1.

Circ Breaker	Class A hits (%)	Class B hits (%)
3ADD10C	79,62	79,24
3ADD30A	100	98,47
3ADD30B	96,98	98,3

A comparison between the separability of classes from the three circuit breakers can be done through the interpretation of Fig. 6, in which a 10-second audio SSCEV from each circuit breaker (not the samples, as done previously) can be found.

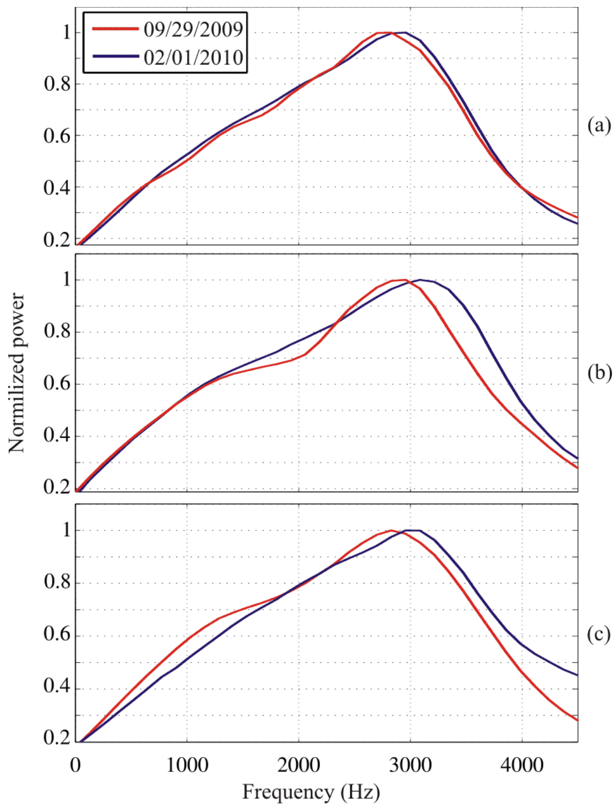

Fig. 6: SSCEV obtained from 10 s audio recorded from circuit breakers in SETPE: (a) 3ADD10C (b) 3ADD30A (c) 3ADD30B.

6 CONCLUSION

In general, the ultrasonic noise originated in equipment with different levels of pollution has shown different spectral decays and peak regions. This behaviour has emphasized the separability of the obtained SSCEV, which facilitated the work of AAANN.

The three proposed approaches have shown encouraging results:

i. In Approach 1, the typical use of the technique was effective.

ii. In the second approach it is shown that, even using only borderline pollution classes for training, the system still provides some reliability.

iii. Approach 3 has shown that the technique also has good results with artificial washing, which was expected. This result reinforces the technique appliance, since patterns obtained before and after artificial washing gave similar results.

Finally, we can say that the estimation of pollution of ceramic electrical insulation from the ultrasonic noise is one step closer to what can be called a reliable monitoring technique.

7 ACKNOWLEDGMENTS

The authors of this paper wish to demonstrate their gratitude to the São Francisco Hydroelectric Company which permitted the access to their facilities, and CNPq, for the scholarships.

Part of the work developed at Substation TermoPE is the result of a research project supported by TermoPernambuco S.A.

8 REFERENCES

[1] L. E. Lundgaard: Partial discharge XIV: Acoustic partial discharge detection - Practical application. IEEE Electrical Insulation Magazine, v. 8, p. 34-43, July/August, 1992.

[2] R. S. Gorur, J. T. Burnham, E. A. Cherney: Outdoor Insulators. 1st Ed. ed. Phoenix: Ravi S. Gorur Inc., 1999.

[3] K. L. Wong, S. Shihab: Radiating signal model for broadband acoustic emission from high voltage equipment. Proceedings of the International Conference on Power System Technology. Kunming: [s.n.]. 2002. p. 1859-1862.

[4] B. Gajić, K. K. Paliwal: Robust Parameters for Speech Recognition Based on Subband Spectral Centroid Histograms, in IEEE Transactions on Audio, Speech, and Language Processing, vol. 14, no. 2, pp.600-608, March 2006.

[5] H. Kimura, T. Tsumura, M. Yokosuka: Corona in Oil as Part of Commercial-Frequency Circuit. Electrotechnical Journal of Japan, 1940. 90-92.

[6] J. R. Leslie, H. O'Beirne: Radio Noise Studies on Power Lines with the Coronaphone. IEEE Transactions on Power Apparatus and Systems, v. 83, p. 495-500, Maio 1964.

[7] G. A. Dawson et al: The acoustic output of a long spark. Journal of Geophysical Research, v. 73, p. 815-816, 1968.

[8] Y. Yang, G. A. DUMONT: Classification of Acoustic Emission Signals Via Hebbian Feature Extraction. Proceedings of the International Joint Conference on Neural Networks, 1991. p. 113-118.

[9] D. W. Auckland et al: Application of ultrasound to the inspection of insulation. IEE Proceedings Science, Measurement & Technology, v. 143, p. 177-181, May, 1996.

[10] M. Abdel-Salam et al Early detection of weak point in MEEC distribution system. Conference Record of the 2001 IEEE Industry Applications Conference. Thirty-Sixth IAS Annual Meeting. Nanjing: [s.n.]. 2001. p. 2541-2545.

[11] T. Boczar: Identification of a specific type of PD from acoustic emission frequency spectra. IEEE Transactions on Dielectrics and Electrical Insulation, v. 8, p. 598-606, August 2001.

[12] C. M. Pei et al: An acoustic emission method for on-line monitoring the contamination-causing flashover of insulator. Proceedings of the International Conference on Electrical Machines and Systems, 2008. ICEMS 2008. Wuhan: [s.n.]. 2008. p. 817-822.

[13] B. Gajić, K. K. Paliwal: Robust parameters for speech recognition based on subband spectral centroid histograms, in EUROSPEECH-2001, 591-594.

[14] M. Minsky, S. Papert: Perceptrons: an introduction to computational geometry, MIT Press, Cambridge, 1969.

[15] M . Riedmiller, H. Braun: A Direct Adaptive Method for Faster Backpropagation Learning: The RPROP Algorithm, in Proceedings of the IEEE International Conference on Neural Networks, 1993.

[16] D. E. Rumelhart, J. L. McClelland: Parallel distributed processing: exploration in the microstructure of cognition. Cambridge: MIT Press, 1986.

[17] B. L. Kalman, S. C. Kwasny: Why tanh: choosing a sigmoidal function. International Joint Conference on Neural Networks. Baltimore: 1992. p. 578 - 581. ISBN: 0-7803-0559-0.

[18] A. Iversen, N. K. Taylor, K. E. Brown: Classification and verification through the combination of the multi-layer perceptron and auto-association neural networks. Proceedings of the 2005 IEEE International Joint Conference on Neural Networks. IJCNN '05. 2005. p. 1166-1171.